Efficient iterative diagonalization of the Bose-Hubbard model for ultracold bosons in a periodic optical trap

Ágnes Szabados, Péter Jeszenszki, Péter R. Surján

Laboratory of Theoretical Chemistry, Loránd Eötvös University, H-1518 Budapest, POB 32, Hungary

Abstract

Composite electronic systems are sometimes modeled by the Bose-Hubbard Hamiltonian. Iterative solution of this model, yielding a handful of the lowest-lying states is presented. The effect of the Hamiltonian on the trial vector is evaluated in a direct manner. A representation on the basis of sites is adopted, the rate limiting factor being merely the one-body term in such circumstances. The iteration follows the scheme of Davidson and provides exact states and state energies of the model Hamiltonian.

Exponential dependence of the memory requirement on the number of bosons and lattice sites sets the limit of applicability to small systems. Restriction of the maximal occupation of sites is investigated in order to reduce the actual memory need. The energy error introduced this way ranges from negligible (in the strong-coupling limit) to substantial (in the weak-coupling limit).

Keywords: Bose-Hubbard model, iterative diagonalization, direct CI

1. Introduction

Atomic systems are usually considered to be composed of of nuclei and electrons when treated at the theoretical level. Under certain experimental situations however, it is possible to consider an entire atom as a single entity. This not only represents an enormous simplification of the problem, but also permits to export the experience accumulated in electron correlation theory to treat other systems, bosonic gases for example.

The system of laser-cooled and trapped bosonic gases lies in the forefront of current research and offers numerous challenges both for theory and experiment. One of the intriguing aspects of the system is the experimental realization of the quantum phase transition phenomenon[1], that has been the subject of many theoretical studies[2, 3, 4, 5]. For some review articles on the subject, see Refs.[6, 7, 8]. Minima of the optical potential lying thousands of nanometers apart, the one-body term of the Hamiltonian can be well approximated

Email addresses: szabados@chem.elte.hu (Ágnes Szabados), jeszenszki@coulson.chem.elte.hu (Péter Jeszenszki), surjan@chem.elte.hu (Péter R. Surján)

by taking into account the tunneling of atoms only between neighboring sites. This gives rise to the hopping parameter, t of the simplest theoretical model describing the system. Inter-particle interaction occurs via scattering, which – as a first approximation – can be considered to be dominantly of on-site nature. To characterize this repulsion, a single two-body integral – the Hubbard parameter, denoted by U – suffices for a single component gas. The above assumptions lead to the Bose-Hubbard Hamiltonian

$$H \;=\; -\,t\,\sum_{\langle\mu\nu\rangle}\left(\chi_\mu^+\,\chi_\nu \;+\; \chi_\nu^+\,\chi_\mu\right) \;+\; \frac{U}{2}\;\sum_{\mu=1}^{K}\chi_\mu^+\,\chi_\mu^+\,\chi_\mu\,\chi_\mu \tag{1}$$

which represents a widely used model of bosonic atoms in an optical lattice at zero temperature[3]. As noted above, this model suffers from several shortcomings: it neglects all one-body terms except first neighbour ones, all interaction terms except for the on site terms are disregarded. In addition, since each gas atom is treated as a single composite particle, only a single band is accounted for. The underlying basis set of the model consist of local site (Wannier-type) functions, however, they are used only implicitly since all matrix elements of the Hamiltonian are semi-empirical parameters.

These shortcomings may result the Bose-Hubbard model rather approximative, depending on the situation at hand. For comparison with numerically exact solutions of the full many-body Schrödinger equation, see Refs. [9, 10, 11].

Operators χ_μ^+ (χ_μ) in Eq.(1) create (annihilate) an atom on site μ and follow standard bosonic algebra

$$\begin{aligned}\left[\chi_\mu^+,\chi_\nu^+\right] &= 0\;,\\ \left[\chi_\mu,\chi_\nu\right] &= 0\;,\\ \left[\chi_\mu^+,\chi_\nu\right] &= \delta_{\mu\nu}\;.\end{aligned}$$

On the right hand side of Eq.(1) $\langle\mu\nu\rangle$ denotes a restriction to neighboring sites with $\nu<\mu$, and K stands for the number of sites in the lattice. Tunability of the system is offered by the fact that variation of the laser intensity (V_0) used for shaping the optical trap has an opposite effect on parameters t and U. Both parameters exhibit an exponential dependence on V_0, the former with negative the latter with positive exponent[1, 3]. As a consequence, both large and small regimes in the ratio U/t are realizable experimentally, by simply altering the laser intensity. The nature of the wavefunction is ultimately different in the weak coupling *i.e.* $U/t\to 0$ limit, and in the strong coupling *i.e.* $U/t\to\infty$ limit.

In both limits the ground state of the system can be approximated by a single symmetric product of one-particle functions, called a permanent, the analogue of a determinant. In the weak coupling regime $U << t$, one can assume that in the ground state all particles occupy the same, system-wide delocalized orbital, φ_0. The many-body wavefunction is given by

$$\Psi_{\rm GP} \;=\; \frac{1}{\sqrt{N!}}\left(\varphi_0^+\right)^N|{\rm vac}\rangle\;. \tag{2}$$

In the $t << U$, strong coupling regime the permanent with equal occupation of all sites gives a good characterization of the ground state. If $n = N/K$ is an integer,

$$\Psi_{\rm MI} \;=\; \frac{1}{(n!)^{K/2}} \prod_{\mu=1}^{K} \left(\chi_\mu^+\right)^n |{\rm vac}\rangle \;. \tag{3}$$

The Mott-insulator wavefunction of Eq.(3) becomes exact if $t = 0$, while the superfluid function Eq.(2) is the exact solution of the model for $U = 0$. Orbital φ_0 appearing in permanent Eq.(2) is derived by minimizing the expectation value of H evaluated with $\Psi_{\rm GP}$, while keeping φ_0 normalized. This leads to a Gross-Pitaevskii (GP) type equation[12], the bosonic analogue of the fermionic Hartree-Fock type self-consistent-field equations:

$$\hat{G}(\varphi_0)\;|\varphi_0\rangle \;=\; \mu_0\;|\varphi_0\rangle\;, \tag{4}$$

with

$$\hat{G}(\varphi_0) \;=\; -\,t\,\sum_{\langle\mu\nu\rangle}\left(\chi_\mu^+\,\chi_\nu \,+\, \chi_\nu^+\,\chi_\mu\right) \,+\, U(N-1)\,\sum_{\mu=1}^{K} |c_{\mu 0}|^2 \chi_\mu^+\,\chi_\mu\;,$$

and

$$\varphi_0^+ \;=\; \sum_{\mu=1}^{K} c_{\mu 0}\,\chi_\mu^+ \tag{5}$$

Apart from the ground-state orbital φ_0, the GP equation (4) provides excited one-particle states $\varphi_i\;,\; i = 1, \ldots, K-1$ as well.

As the ratio U/t leaves the extreme ranges $\sim \infty$ or ~ 0, the MI or the GP permanent becomes less appropriate, inducing the development of refined approximations. Still in the single permanent framework, a best mean-field approach has been investigated[13] characterized by the wavefunction

$$\Psi_{\rm BMF} \;=\; \prod_{i=1}^{K} \frac{1}{\sqrt{n_i!}} \left(\varphi_i^+\right)^{n_i} |{\rm vac}\rangle\;, \tag{6}$$

with orbitals φ_i and occupation numbers n_i determined based on the variation principle, with proper orthonormality constraints. Beyond mean-field approximations for trapped bosonic systems have lived a rapid progress recently. The techniques applied include several strategies well known from the field of molecular electron-correlation, like restricted configuration interaction (CI)[14, 15, 16, 17], coupled-cluster (CC)[18], multi-configurational self-consistent field[19] or the random phase approximation for excitation energies[14]. Another important scheme is multiconfigurational time-dependent Hartree method for bosons (MCTDHB) [31, 32]. Most of these methods, in principle, allow to obtain numerically exact solutions of the many-body Schröedinger equation.

Density Matrix Renormalization Group (DMRG) has become a widespread tool to approximate systematically the solution of the given model[20, 21]. An alternative, less popular approach is the iterative diagonalization of the matrix **H** built in the Hilbert space of permanents. Preference for DMRG lies with its polynomial scaling with N and K. It also offers fast convergence for 1D chains and for 2D lattices in some circumstances. Favourable scaling of DMRG is due to the fact, that the exact wavefunction expanded on the basis of all permanents Φ_I:

$$\Psi \;=\; \sum_I c_I \, \Phi_I \tag{7}$$

is never constructed explicitly. At comparison with DMRG, iterative diagonalization shows exponential scaling, since the length of the above expansion (the dimension of the Hilbert space for N particles and K sites) is given by

$$\mathcal{D}(N,K) \;=\; \frac{(N+K-1)!}{N!(K-1)!} \;=\; \binom{N+K-1}{K-1} \, . \tag{8}$$

It is apparent that the dimensionality of the full CI problem of the bosonic Hamiltonian is even more severe than that of the fermionic case. This would render iterative algorithms prohibitive, but for efficient numerical procedures applicable during the computation. To reduce the computational demand, it is typical to exploit the spatial symmetry of the lattice and take into account the sparsity of the Hamiltonian[15, 20, 22, 23, 24]. It has also been emphasized recently, that the direct algorithm introduced by Roos et al[25]. can be exploited to lift the need of storing the Hamiltonian matrix[16, 17, 26]. Though approximate DMRG calculations are cheaper, iterative diagonalization algorithms offer the advantage of stable convergence, irrespective of the parameter ratio U/t. This makes them proper benchmark techniques, whenever a validation or error analysis is required. We note that techniques to solve the Schrödinger equation numerically exactly are also available [27, 28, 29, 30, 31, 32].

In the present study we apply the direct CI technique to compute the ground state of finite-size square lattices at zero Kelvin, filled with a moderate number of atoms. Key ingredients of the iterative diagonalization algorithm are (i) an enumeration scheme identifying the permanents, (ii) evaluation of the **Hc** product and (iii) an iteration procedure relying merely on **c** and **Hc** vectors. All ingredients have been known before, still, to our knowledge, they have not got combined yet for the exact solution of the Bose-Hubbard model. Technically similar calculations were performed by Sundholm and Vänskä[16], who performed direct configuration interaction calculations in the GP basis set, for bosonic particles with coulomb interactions.

The time consuming step of the algorithm is the action of **H** on a trial vector **c**. To enhance rapid computation of the **Hc** product, both quantities are expressed via site-centered orbitals χ_μ. Though this basis may not be appropriate with truncated CI expansions[19], site-centered orbitals are preferable in the full CI case, since the two-body term of Eq.(1) is of on-site nature. Consequently, on the basis of χ_μ's, the one-body term of Eq.(1) becomes the rate determining factor of an iteration step, while evaluation of the two-body term

is cost-less in comparison – a situation quite intriguing and embarrassing for a quantum chemist.

Apart from full CI solutions, truncation of the Hilbert space is also investigated, with a restriction imposed on the maximal occupation of lattice sites. Considering M atoms ($M < N$) at a site at maximum, the length of expansion Eq.(7) is reduced to[8]

$$\mathcal{D}_M(N,K) \;=\; \sum_{j=0}^{\left[\frac{N}{K+1}\right]} (-1)^j \binom{M+N-1-j\,(K+1)}{M-1} \binom{M}{j}\,, \tag{9}$$

bringing larger systems into the reach of iterative diagonalization. In the above, [.] denotes the floor function. Working with restricted site occupation necessitates an enumeration algorithm adapted for the truncated Hilbert space. Such an algorithm is introduced below.

In what follows the iterative diagonalization technique is presented briefly, followed by numerical applications. The numerical examples focus on demonstrating the efficiency and usefulness of the direct CI technique. It is also shown, that restricting maximal occupation of sites represents a good approximation only in the strong-coupling limit.

2. Theory

2.1. Enumeration of permanents

A permanent Φ_I appearing in expansion Eq.(7) can be expressed in the form

$$\Phi_I \;=\; \prod_{\mu=1}^{K} \frac{1}{\sqrt{n_\mu!}} \left(\chi_\mu^+\right)^{n_\mu} |\mathrm{vac}\rangle \tag{10}$$

with $\sum_{\mu=1}^{K} n_\mu = N$. Obviously, Φ_I is in one to one correspondence with the occupation vector

$$\mathbf{n}^I \;=\; (n_1, n_2, \ldots, n_K)\ .$$

Our aim here, is to associate an index I with the above vector. This is usually achieved through the lexicographical ordering of occupation vectors, which provides an indexing without gaps[16, 23]. Streltsov et al. made use of the combinadic representation of integers, which also leads to the lexicographical indexing of the above permanents[26]. An alternative ordering is presented below, which leads to an addressing scheme different from the lexicographical. However, the indexing has no relevance to the physics of the problem, and the two schemes yield the same computational demand when computing the **Hc** product.

The ordering of occupation vectors for K lattice sites and N particles is achieved by the following algorithm:

$I = 1$
$n_1 = N$ `and` $n_2 = \cdots = n_K = 0$
`start with` $\mathbf{n}_1 = (N, 0, \ldots, 0)$

```
1       I = I + 1
        if n_1 > 0 then
           n_1 = n_1 − 1 and n_2 = n_2 + 1
           n_I = (n_1, n_2, ...)
           goto 1
        endif
        if n_1 = 0 then
           let i be the smallest site index, for which n_i ≠ 0
           if i = K goto 2
           n_i = 0, n_{i+1} = n_{i+1} + 1 and n_1 = n_i − 1
           n_I = (n_1, n_2, ...)
           goto 1
        endif
2       end
```

An illustration for the case $K = N = 3$ is shown is Table 1.

Once the ordering is set, permanent (10) is conveniently addressed by its serial number in the ordered list. To compute the address, it is practical to introduce the summed occupation of sites with indices larger than μ:

$$s_\mu \;=\; \sum_{\nu=\mu+1}^{K} n_\nu$$

The next step is to define quantity I_μ

$$I_\mu \;=\; \sum_{i=0}^{n_\mu-1} \mathcal{D}(N - s_\mu - i, \mu - 1) \;=\; \binom{N - s_\mu - i + \mu - 2}{\mu - 2} \tag{11}$$

which gives the number of permanents occurring in the ordered list before the occupation of site μ gets n_μ, for $N - s_\mu$ particles and μ sites. In fact index vector

$$\mathbf{I} \;=\; (I_1, I_2, \ldots, I_K)$$

is in one to one correspondence with permanent (10), just like the occupation vector. Index vector $\mathbf{I}$ is in direct relation with the serial number I, which can be expressed as

$$I \;=\; 1 \;+\; \sum_{\mu=1}^{K} I_\mu \tag{12}$$

2.2. Enumeration with restricted site occupation

Since the dimension of the full configuration space grows factorially with N and K, it is of practical concern to reduce the number of permanents appearing in expansion Eq.(7). In the CI framework, restriction according to excitation level is common, which however

suffers from the size-consistency problem[33]. Via the exponential parametrization, coupled cluster approach keeps the number of parameters small, but assumes (though never explicitly constructs) the wavefunction expanded in the full CI space. As a benefit, size-consistency holds for the CC method when working with fermions. Interestingly, size-consistency of truncated CC is violated for the bosonic algebra, though the error is shown to be small if dividing the supersystem for large ($N \gg 1$) fragments[18].

In the present study, we explore a truncation in the CI space, based on site occupations. It is interesting to note, that no analogous truncation is possible in a fermionic CI, where site occupations are limited by 1 anyway, due to the Pauli principle. This approach is motivated by the fact that the single permanent Eq.(3) is not appropriate even for $t = 0$, if N/K is non-integer. In such a case, the simplest approximation on the basis of sites is a linear combination of permanents with occupation numbers $[n/K]$ and $[n/K] + 1$. Due to the large on-site repulsion, occupation numbers are not expected rise much above $[n/K] + 1$ in the strong coupling limit. Hence, restricting maximal site occupation is reasonable for this parameter range. Moreover, restriction on maximal site occupation is harmless from the size-consistency point of view, since this characteristic is not altered when extending a system or dividing it for fragments. (Although this statement seems to be plausible, we have verified it by control calculations: Using $U/t = 6.0$ for two non-interacting chain of 4 sites and 4 atoms each, the exact eigenvalue of the Bose-Hubbard Hamiltonian is -3.771512. Restricting the maximal occupation to 2, we got -3.653360, which is exactly twice of -1.826680, the energy of one subunit with the same maximal occupancy.)

To extend the enumeration scheme for the restricted case, let us first study the expression

$$R(x) \;=\; \left(\sum_{N=0}^{M} x^N\right)^K \;=\; \sum_{N=0}^{M\cdot K} C(N,K)\, x^N \;. \tag{13}$$

We wish to calculate coefficients $C(N,K)$ appearing in the K'th power of the sum of M terms. This can be done in a recursive fashion, similar to generating the binomials to form Pascal's triangle. The recursion rule can be deduced by writing $R(x)$, the so-called generating function as

$$\begin{aligned}
R(x) &= \left(1 + x + \cdots + x^M\right)^{K-1} \left(1 + x + \cdots + x^M\right) \\
&= \left(\cdots + C(N-M, K-1)\, x^{N-M} + C(N-M+1, K-1)\, x^{N-M+1} + \ldots \right. \\
&+ \left. C(N, K-1)\, x^N + \ldots\right) \left(1 + x + ... + x^M\right) \\
&= \ldots + \underbrace{\left(C(N-M, K-1) + C(N-M+1, K-1) + \ldots + C(N, K-1)\right)}_{C(N,K)}\, x^N + \ldots
\end{aligned}$$

Introducing lower index M, the recursion rule for $C_M(N,K)$ is given by

$$C_M(N,K) \;=\; \sum_{L=N-M}^{N} C_M(L, K-1) \;. \tag{14}$$

Quantity $C_M(N,K)$ is to be regarded zero if condition $0 \le N \le M \cdot K$ does not hold. To start the recursion, the initial value $C_M(0,0) = 1$ has to be applied. As indicated by Fig. 1, quantities $C_M(N,K)$ are conveniently arranged into a generalized Pascal's triangle, for a given M. In the triangle, $K+1$ gives the row index and $N+1$ the column index. In fact, case $M = 1$ corresponds to the ordinary Pascal triangle. For $M < N$, quantity $C_M(N,K)$ gives the dimension of the CI space with occupation of sites restricted to M at maximum:

$$\mathcal{D}_M(N,K) \;\; = \;\; C_M(N,K) \; . \tag{15}$$

From the computational point of view, calculation of $\mathcal{D}_M(N,K)$ is preferably done via Eqs.(15) and (14) than by multiplying and summing binomials according to Eq.(9). For this reason, our computations start by generating the generalized Pascal's triangle up till the row needed, to be utilized for addressing. Memory and processor time spent on the triangle is negligible as compared to the storage of the CI vector and calculation of **Hc**.

Next, the ordering of occupation vectors obeying the restriction is needed. This is achieved by the following modification of the previous algorithm:

```
I = 1
n_1 = ··· = n_[N/M] = M ,  n_[N/M]+1 = N − M ∗ [N/M]  and  n_[N/M]+2 = ··· = n_K = 0
start with n_1 = (n_1, n_2, ..., 0)
1       I = I + 1
        if  n_1 > 0  then
            δ = 0
            if  n_1 < M  then
                δ = M − n_1
                n_1 = M
            endif
            let i be the smallest site index, for which n_i < M  and  i > 1
            n_i = n_i + 1 ,  n_i−1 = n_i−1 − 1 − δ
            n_I = (n_1, n_2, ... )
            goto 1
        endif
        if  n_1 = 0  then
            let j be the smallest site index, for which n_j > 0  and  j > 1
            let i be the smallest site index, for which n_i < M  and  i > j
            if no such i exists goto 2
            n_i = n_i + 1 ,  n_i−j = n_j − 1
            if  (i − j − 1) > 0  then  n_i−j−1 = n_i−j−2 = ··· = n_1 = M
            n_i−j+1 = n_j−k+2 = ··· = n_j−1 = 0
            n_I = (n_1, n_2, ... )
            goto 1
        endif
2       end
```

An illustration for the case $K = N = 3$ and $M = 2$ is shown is Table 1.

Once the CI space dimensions $\mathcal{D}_M(N, K)$ are at hand and the ordering is set, the addressing seen previously can be used. This means expressing I_μ with the elements of the generalized Pascal triangle as

$$I_\mu \;=\; \sum_{i=0}^{n_\mu - 1} \mathcal{D}_M(N - s_\mu - i, \mu - 1) \;,$$

and summing it according to Eq.(12) to give address I of the occupation vector $\mathbf{n}^I$. This strategy is similar to the one used by Schnack et al[34]. in the context of Lanczos diagonalization for spin-systems.

2.3. Acting with the Hamiltonian

Calculating the action of the Hamiltonian on the fly is a very beneficial technique – used for decades by quantum chemists[25, 35] – to spare the storage of the Hamiltonian matrix. Since interest in laser cooled and trapped atomic gases rose, several studies have applied the same technique to compute static[16, 17] and dynamic[36, 37] characteristics of bosonic systems. Recently, Streltsov et al.[26] emphasized the usefulness of the approach, giving the general formulae for one- and two-component fermionic and bosonic systems as well as mixtures of the two.

Below, the expressions for the components of vector

$$\boldsymbol{\sigma} \;=\; \mathbf{H}\mathbf{c}$$

are given for the case where both $\boldsymbol{\sigma}$ and $\mathbf{c}$ collect the expansion coefficients belonging to permanents built with site-centered orbitals. In this case the Hubbard term of Eq.(1) acts as a multiplicative operator on any permanent. Introducing $\boldsymbol{\sigma}^t$ and $\boldsymbol{\sigma}^U$ for the result of the hopping and Hubbard-term respectively

$$\boldsymbol{\sigma} \;=\; \boldsymbol{\sigma}^t \;+\; \boldsymbol{\sigma}^U \;,$$

component I of $\boldsymbol{\sigma}^U$ is given by

$$\sigma_I^U \;=\; c_I \, \frac{U}{2} \sum_{\mu}^{K} n_\mu^I \left(n_\mu^I - 1 \right) \;. \tag{16}$$

In the above n_μ^I refer to the occupation numbers of the permanent with index I. The hopping term relates two permanents differing by single substitutions, according to

$$\begin{aligned} \sigma_I^t \;&=\; -\,t \sum_{\langle \mu\nu \rangle} \sum_J \langle \Phi_I | \chi_\mu^+ \, \chi_\nu \;+\; \chi_\nu^+ \, \chi_\mu | \Phi_J \rangle \; c_J \\ &=\; -\,t \sum_{\langle \mu\nu \rangle} \left(c_{I + \Delta(I,\mu,\nu)} \;+\; c_{I + \Delta(I,\nu,\mu)} \right) \;, \end{aligned} \tag{17}$$

where $\Delta(I,\mu,\nu)$ is introduced for the difference of the address of permanent $\langle\Phi_I|\chi_\mu^+\,\chi_\nu$ and I. As it is shown below, calculation cost of $\Delta(I,\mu,\nu)$ is proportional to $|\mu-\nu|$. Taking this into account, comparison of expressions Eq.(16) and Eq.(17) clearly reflects the peculiar situation that the one-body term is the rate determining step while the processor time of the two-body is negligible.

Let us now derive the address difference $\Delta(I,\mu,\nu)$. Starting with the occupation vector of permanent I

$$\mathbf{n}^I \;=\; \left(n_1^I, n_2^I, \ldots, n_K^I\right) \;,$$

permanent $\langle\Phi_J| = \langle\Phi_I|\chi_\mu^+\,\chi_\nu$ is characterized by the occupation vector

$$\begin{aligned}\mathbf{n}^J &= \left(n_1^J, n_2^J, \ldots, n_K^J\right)\\ &= \left(n_1^I, n_2^I, \ldots, n_\nu^I+1, \ldots, n_\mu^I-1, \ldots, n_K^I\right) \;,\end{aligned}$$

assuming that $\nu<\mu$. (The reverse case is considered at the end of the Section.) Making use of Eq.(12) the address difference is obtained as

$$\Delta(I,\mu,\nu) \;=\; J-I \;=\; \sum_{\lambda=1}^{K}\left(J_\lambda - I_\lambda\right) \;.$$

Substituting expression of I_λ from Eq.(11) one gets

$$\Delta(I,\mu,\nu) \;=\; \sum_{\lambda=1}^{K}\underbrace{\left(\sum_{j=0}^{n_\lambda^J-1}\mathcal{D}(N-s_\lambda^J-j,\lambda-1) \;-\; \sum_{i=0}^{n_\lambda^I-1}\mathcal{D}(N-s_\lambda^I-i,\lambda-1)\right)}_{\Delta(I,\mu,\nu,\lambda)} \;. \quad (18)$$

Since occupation numbers n_λ^J as well as summed occupation numbers s_λ^J match for indices J and I, the above two terms cancel if $\lambda<\nu$ or $\mu<\lambda$. The sum in Eq.(18) therefore can be restricted for $\lambda\in[\nu,\mu]$. Evaluating the three distinct cases results:

- case $\lambda=\nu$

$$\Delta(I,\mu,\nu,\nu) \;=\; \sum_{j=0}^{n_\nu^I}\mathcal{D}(N-s_\nu^I+1-j,\nu-1) \;-\; \sum_{i=0}^{n_\nu^I-1}\mathcal{D}(N-s_\nu^I-i,\nu-1) \;.$$

  Substituting $i=j-1$ in the first term one arrives to:

$$\Delta(I,\mu,\nu,\nu) \;=\; \mathcal{D}(N-s_\nu^I+1,\nu-1) \;.$$

- case $\nu < \lambda < \mu$

$$\Delta(I,\mu,\nu,\lambda) \;=\; \sum_{j=0}^{n_\lambda^I-1} \mathcal{D}(N-s_\lambda^I+1-j,\lambda-1) \;-\; \sum_{i=0}^{n_\lambda^I-1} \mathcal{D}(N-s_\lambda^I-i,\lambda-1)$$

Substituting $i = j-1$ in the first term one arrives to:

$$\Delta(I,\mu,\nu,\lambda) \;=\; \mathcal{D}(N-s_\lambda^I+1,\lambda-1) \;-\; \mathcal{D}(N-s_{\lambda-1}^I+1,\lambda-1)$$

- case $\lambda = \mu$

$$\begin{aligned}\Delta(I,\mu,\nu,\mu) &= \sum_{j=0}^{n_\mu^I-2} \mathcal{D}(N-s_\mu^I-j,\mu-1) \;-\; \sum_{i=0}^{n_\mu^I-1} \mathcal{D}(N-s_\mu^I-i,\mu-1) \\ &= -\,\mathcal{D}(N-s_{\mu-1}^I+1,\mu-1)\end{aligned}$$

Substitution of the above results into Eq.(18) finally yields:

$$\begin{aligned}\Delta(I,\mu,\nu) &= \mathcal{D}(N-s_\nu^I+1,\nu-1) \\ &+ \sum_{\lambda=\nu+1}^{\mu-1} \left(-\mathcal{D}(N-s_{\lambda-1}^I+1,\lambda-1) \;+\; \mathcal{D}(N-s_\lambda^I+1,\lambda-1)\right) \\ &- \mathcal{D}(N-s_{\mu-1}^I+1,\mu-1) \qquad (19)\end{aligned}$$

Equation (19) is the working formula for $\Delta(I,\mu,\nu)$ if a restriction on site occupations is applied.

In the unrestricted case, it is possible to further simplify Eq.(19) if substituting the binomials for dimensions $\mathcal{D}$ as indicated in Eq.(11). Making this step reveals, that the right hand side of Eq.(19) is a telescopic sum: its terms can be pairwise simplified to give one term. As an example, the simplification of the first two terms look:

$$\binom{N-s_\nu^I+\nu-1}{\nu-2} \;-\; \binom{N-s_\nu^I+\nu}{\nu-1} \;=\; -\binom{N-s_\nu^I+\nu-1}{\nu-1}$$

where the well known relation for binomial coefficients is used in the form

$$\binom{a+b}{b} \;-\; \binom{a+b+1}{b+1} \;=\; -\binom{a+b}{b+1}\,.$$

Upon simplification, Eq.(19) takes the form

$$\Delta(I,\mu,\nu) \;=\; -\sum_{\lambda=\nu+1}^{\mu} \binom{N-s_{\lambda-1}^I+\lambda-2}{\lambda-2}\,. \qquad (20)$$

The binomial relation can also be applied for the $M = 1$ restricted case to simplify Eq.(19), it is however of little practical relevance.

In addition to $\Delta(I, \mu, \nu)$, the address difference $\Delta(I, \nu, \mu)$ is also needed for each index pair $\nu < \mu$. If wishing to calculate $\Delta(I, \nu, \mu)$, it is not necessary to repeat the derivation. Realizing that the relation $\langle \Phi_J | = \langle \Phi_I | \chi_\mu^+ \chi_\nu$ implies $\langle \Phi_I | = \langle \Phi_J | \chi_\nu^+ \chi_\mu$, one can write

$$\Delta(J, \nu, \mu) \;=\; I - J \;=\; -(J - I) \;=\; -\,\Delta(I, \mu, \nu)\ .$$

Based on the relation $s_\lambda^I = s_\lambda^J + 1$ for $\nu \leq \lambda < \mu$ and using Eq.(20), the difference can be expressed as

$$\Delta(J, \nu, \mu) \;=\; \sum_{\lambda=\nu+1}^{\mu} \binom{N - s_{\lambda-1}^J + \lambda - 3}{\lambda - 2}$$

which holds for any index J and $\nu < \mu$, in the unrestricted site occupation case. For $M < N$ the expression derived from Eq.(19)

$$\begin{aligned}
\Delta(J, \mu, \nu) \;&=\; -\,\mathcal{D}(N - s_\nu^J, \nu - 1) \\
&+\; \sum_{\lambda=\nu+1}^{\mu-1} \left(\mathcal{D}(N - s_{\lambda-1}^J, \lambda - 1) \;-\; \mathcal{D}(N - s_\lambda^J, \lambda - 1)\right) \\
&+\; \mathcal{D}(N - s_{\mu-1}^J, \mu - 1)
\end{aligned}$$

applies. We conclude the Section by mentioning that calculation of $\Delta(I, \nu, \mu)$ requires $2|\mu - \nu|$ additions in the restricted case. In the unrestricted case there is a factor of 2 gained by the telescopic sum, yielding a cost proportional to $|\mu - \nu|$. This agrees with the number of additions necessary for getting $\Delta(I, \nu, \mu)$ if using the addressing Eq.(20) of Streltsov et al.[26]

2.4. Transformation of the GP vector to the site basis

To utilize the simplicity of the two-body term, it is mandatory to carry out the calculation in the site basis set. However, in a wide range of U/t values a good initial guess to the iterative CI is provided by the GP function (2). To find the expression of this wavefunction in the site basis, Eq.(5) is substituted into the GP function (2):

$$\Psi_{\mathrm{GP}} \;=\; \frac{1}{\sqrt{N!}} \left(\sum_{\mu=1}^{K} c_{\mu 0}\, \chi_\mu^+ \right)^N |\mathrm{vac}\rangle\ .$$

Writing the sum for two terms, $\mu = 1$ and the rest, one gets the binomial expansion

$$\Psi_{\mathrm{GP}} \;=\; \frac{1}{\sqrt{N!}} \sum_{\nu_1=0}^{N} \binom{N}{\nu_1} c_{10}^{\nu_1} \left(\chi_1^+\right)^{\nu_1} \left(\sum_{\mu=2}^{K} c_{\mu 0}\, \chi_\mu^+ \right)^{N-\nu_1} |\mathrm{vac}\rangle\ .$$

Repeating this derivation step till there remain terms under the brackets, the formula

$$\Psi_{\mathrm{GP}} = \frac{1}{\sqrt{N!}} \sum_{\nu_1=0}^{N} \sum_{\nu_2=0}^{N-\nu_1} \cdots \sum_{\nu_K=0}^{N-\sum_{i=1}^{K-1}\nu_i} \binom{N}{\nu_1} \binom{N-\nu_1}{\nu_2} \cdots \binom{N-\sum_{i=1}^{K-1}\nu_i}{\nu_K} c_{10}^{\nu_1} c_{20}^{\nu_2} \cdots c_{K0}^{\nu_K} \left(\chi_1^+\right)^{\nu_1} \left(\chi_2^+\right)^{\nu_2} \cdots \left(\chi_K^+\right)^{\nu_K} |\mathrm{vac}\rangle \ .$$

is resulted. Coefficient c_I associated with occupation vector $\mathbf{n}^I = (\nu_1, \nu_2, \ldots, \nu_K)$ can be directly read from the above and easily coded.

3. Numerical tests

A few illustrative examples are presented below to show the usefulness and limits of the iterative diagonalization approach for bosonic systems.

There exist two widespread algorithms for the generation of a few eigenvectors via the repeated action of the Hamiltonian on a trial vector, one introduced by Lanczos[38], the other by Davidson[39]. Both can be combined with the direct action of the Hamiltonian. In the present study we apply Davidson's technique.

In the weak coupling regime we use the GP solution as initial vector, transformed into the site basis, as described in Section 2.4. As the ratio U/t is increased, it becomes difficult to get the GP iteration converged. In this parameter range, orbital φ_0 is constructed as

$$\varphi_0 = \frac{1}{\sqrt{K}} \sum_{\mu=1}^{K} \chi_\mu \ ,$$

and used to build the permanent of Eq.(2) to get transformed subsequently into the site basis.

Obtaining a few excited states is also possible by Davidson's method. Iterating for excited states brings an increase in calculation time, but should not pose any technical problem. In the present paper, however, we focus on the ground state.

Efficiency of the iterative diagonalization is demonstrated on Fig. 2, by comparing the memory need and the computation time of the present algorithm with the sparse Lanczos method implemented in the open source ALPS package[40, 41]. In the latter approach sparse linear algebra routines are used to store matrix $\mathbf{H}$ and compute the product $\mathbf{Hc}$. As Fig. 2 reflects, handling only the nonzero elements of $\mathbf{H}$ brings a reduction in system memory by two orders of magnitude at least. Memory requirement is further reduced by about another two orders of magnitude if applying the direct action of the Hamiltonian. To estimate whether direct iteration is feasible for a system, double precision storage of two vectors of the dimension of the Hilbert space (full or restricted) is to be considered. The calculations presented in this study are performed on ordinary PC-s. The largest system among our examples (presented in Table 3) is built of 16 sites and 16 particles, giving a CI space of $3 \cdot 10^8$ permanents, and allocating 4.5 Gigabyte computer memory during computation.

Comparison of computation times presented in Fig. 2b only serves an illustrative purpose. Though the Lanczos and direct diagonalization calculations were performed on the same machine (supplied with an AMD Phenom(tm) II X4 925 processor), the ALPS source is far from being optimized for the present problem. It rather intends to be a program package applicable for a wide range of model Hamiltonians. It may be possible, that the time gain reflected by Fig. 2b is attributable to the overhead needed by the indexing of sparse routines. Still, further tests are needed to investigate this question, preferably done with the sparse and direct routines embedded in the same code. We mention here, that ideal computation time of the direct iteration by Davidson's algorithm is obtained if vectors forming the Davidson subspace can be stored in page cache. Otherwise, the algorithm necessitates live disk I/O during computation, which considerably slows down the iteration time.

In the next example, the effect of restricting maximal site occupation is investigated, on the example of a lattice of 3×3 sites, filled with $N = 9$ particles. In Fig. 3 expectation value of site occupations

$$n_\mu \;=\; \langle\Psi|\chi_\mu^+\chi_\mu|\Psi\rangle \;=\; \sum_I c_I^2\, n_\mu^I \tag{21}$$

is depicted for the three topologically different sites: central, on the edge and on the corner. Variance of site occupations, computed by

$$\sigma_\mu \;=\; \sqrt{\langle\Psi|\chi_\mu^+\chi_\mu\chi_\mu^+\chi_\mu|\Psi\rangle - \langle\Psi|\chi_\mu^+\chi_\mu|\Psi\rangle^2} \;=\; \sqrt{\sum_I {n_\mu^I}^2 c_I^2 - \left(\sum_I n_\mu^I c_I^2\right)^2} \tag{22}$$

is plotted in Fig. 4 for the above three cases.

Both quantities reflect the characteristic change of the system when passing from the weak-coupling to the strong-coupling regime. For small U/t values site occupations are apparently uneven, particles favouring the central position due to the energy gain brought about by the hopping term. At parallel with this, variance of site occupations is also large in the weak-coupling range, indicating that large fluctuations are present in the system, particles move easily along the lattice. As U/t is increased, occupation numbers level out and density fluctuations drop, the latter tending to 0 in the limit $U \to \infty$ for this system. Examining the effect of restricting maximal site occupation, no significant change is spotted for $U/t > 10$. Below this value, drastic reduction of maximal site occupation to $M = 1$ or $M = 2$ introduces a significant error, flattening out the site occupation map and reducing density fluctuations. In the $U = 0$ limit the error introduced in site occupation amounts to a rough 100 % for $M = 1$ for the central and the corner sites, while it is about 35 % for $M = 2$. The effect on occupation number variance is less expressed, the error amounts to about 50 % for the central site for $M = 1$ and to about 30 % for $M = 2$. Insets in the figures demonstrate the diminishing of the error as the value of M gets larger: the $M = 6$ curve can not be distinguished from the exact one even in the weak-coupling regime.

It is interesting to study a further characteristic of the system, the so-called condensate fraction, f_c obtained as

$$f_c \;=\; \lambda_1/N\ .$$

Here λ_1 is the largest eigenvalue of the first order density matrix

$$\rho_{\mu\nu} \;=\; \langle\Psi|\chi_\mu^+\chi_\nu|\Psi\rangle \;=\; \sum_I c_I\, c_{I+\Delta(I,\mu,\nu)} \;.$$

The condensate fraction is depicted in Fig. 5, and shows hardly any change as the restriction on maximal site occupation is lowered to as small value, as $M = 2$. The insensitivity of f_c to restricting the maximal site occupation implies, that checking the Penrose-Onsager criterion[42] may be possible for relatively large systems, via reducing the value of M.

Checking the raise in energy obtained when restricting site occupation offers another measure of the error committed. These data are collected in Table 2, showing orders of magnitude difference for a given M value in the weak- and strong-coupling situation. There is only a factor of 10 difference in error percentages for the extreme low value $M = 2$, while at $M = 3$ the error drops to the order 10^{-2} % in the weak-coupling range. This is to be compared to the cca. 8 % error in the strong coupling range, which can be considered substantial.

Finally, we investigate the sparsity of the wavefunction on the example of a 4×4 lattice, with $N = 16$ particles, at different parameter ratios. The number of nonzero components of the wavefunction collected in Table 3 is intimately connected with the diagonal nature of the first order density matrix. As a measure of this latter feature, the averaged diagonal to off-diagonal ratio denoted by r, is also shown in the table. In the limit $U \to \infty$, r also tends to infinity as the density matrix written on the site basis becomes diagonal. The onset of this behaviour is already detectable in the value of r as the parameter ratio is increased from 0.1 to 10. At the same time, the CI vector becomes less populated in the coefficient range $10^{-5} - 10^{-6}$, the majority of the components gradually dropping in the range 10^{-6} or less. In parallel with this, the number of components falling in the range $10^{-1} - 10^{-3}$ considerably increases. This indicates, that a sparse CI algorithm combined with the direct calculation of the **Hc** product, similar to the one recently developed in the many-electron framework[43], may be beneficial for these systems too.

4. Conclusion

Summarizing, efficient evaluation of the action of the Bose-Hubbard Hamiltonian on a trial vector, as recently emphasized by Streltsov et al.[26], has been exploited to set up an iterative diagonalization procedure. A new code has been written, which produces exact states and energies of the Bose-Hubbard model for small lattices and particle numbers, providing a benchmark utility. The code performing the iterative diagonalization for the Bose-Hubbard model is a standalone program, written in FORTRAN 90. The source is available upon request.

Quantities used for grabbing the superfluid or Mott-insulator character of the wavefunction, like site occupation, occupation variance, or natural populations are available in the existing code. Address relation of single substitutions given in Eqs.(19) and (20) permit an easy coding of any further quantity expressible as an expectation value of a one-particle operator.

5. Dedication

This paper is dedicated to Professor Debashis Mukherjee, whose broad scientific interest combined with his open personality permanently stimulates us, just like many other friends of him. We have discussed several times on cooled and trapped bosonic atoms as a possible new field of research, where accumulated knowledge of our hinterland can be exported to.

6. Acknowledgments

The authors express their thanks to professor B. Das (Bangalore, India) who drew their attention to the subject of laser cooled bosons in optical traps.

This work has been supported by the Hungarian National Research Fund (OTKA), grant numbers K-81588 and K-81590. The European Union and the European Social Fund have also provided financial support to the project under the grant agreement ??TÁMOP 4.2.1./B-09/1/KMR-2010-0003.

The sparse Lanczos results were produced by the open source ALPS codes for strongly correlated systems, release 1.3.[40, 41]

[1] M. Grenier, O. Mandel, T. Esslinger, T. Hänsch, I. Bloch, Nature 415 (2002) 39.
[2] M. Fisher, P. Weichman, G. Grinstein, D. Fisher, Phys. Rev. B 40 (1989) 546.
[3] D. Jaksch, C. Bruder, J. Cirac, C. Gardiner, P. Zoller, Phys. Rev. Letters 81 (1998) 3108.
[4] M. Aizenman, H. Lieb, R. Seiringer, J. P. Solovej, J. Yngvason, Phys. Rev. A 70 (2004) 023612.
[5] B. Caprogrosso-Sansone, N. V. Prokof'ev, B. V. Svistunov, Phys. Rev. B 75 (2007) 134302.
[6] O. Morsch, M. Oberthaler, Rev. Mod. Phys. 78 (2006) 179.
[7] I. Bloch, J. Dalibard, W. Zwerger, Rev. Mod. Phys. 80 (2008) 885.
[8] M. Lewenstein, A. Sanpera, V. Ahufinger, B. Damski, A. Sen(De), U. Sen, Adv. Phys. 56 (2007) 243–379.
[9] K. Sakmann, A. I. Streltsov, O. E. Alon, L. S. Cederbaum, Phys. Rev. Letters 103 (2009) 220601.
[10] K. Sakmann, A. I. Streltsov, O. E. Alon, L. S. Cederbaum, Phys. Rev. A 82 (2010) 013620.
[11] K. Sakmann, A. I. Streltsov, O. E. Alon, L. S. Cederbaum, New J. Phys. 13 (2011) 043003.
[12] F. Dalfovo, S. Giorgini, L. Pitaevskii, S. Stringari, Rev. Mod. Phys. 71 (1999) 463–512.
[13] O. E. Alon, A. I. Streltsov, L. S. Cederbaum, Phys. Lett. A 347 (2005) 88???94.
[14] B. D. Esry, Phys. Rev. A 55 (1997) 1147.
[15] T. Haugset, H. Haugerud, Phys. Rev. A 57 (1998) 3809.
[16] D. Sundholm and T. Vänskä, J. Phys. B 37 (2004) 2933–2942.
[17] T. Vänskä and D. Sundholm and M. Lindberg, Phys. Rev. A 75 (2007) 023621.
[18] L. S. Cederbaum, O. E. Alon, A. I. Streltsov, Phys. Rev. A 73 (2006) 043609.
[19] A. I. Streltsov, O. E. Alon, L. S. Cederbaum, Phys. Rev. A 73 (2006) 063626.
[20] R. M. Noack, S. R. Manmana, AIP Conf. Proc. 789 (2005) 93–163.
[21] S. Ramanan, T. Mishra, M. S. Luthra, R. Pai, B. P. Das, Phys. Rev. A 79 (2009) 013625.
[22] E. Lundh, Phys. Rev. A 70 (2004) 033610.
[23] J. M. Zhang, R. X. Dong, Eur. J. Phys 31 (2010) 591–602.
[24] M. A. E. Leung, W. P. Reinhardt, Comput. Phys. Commun. 177 (2007) 348–356.
[25] B. Roos, P. Siegbahn, in: H. Schaefer (Ed.), Modern Theoretical Chemistry, vol. 3, chap. 7, Plenum, New York, 1977.
[26] A. I. Streltsov, O. E. Alon, L. S. Cederbaum, Phys. Rev. A 81 (2010) 022124.
[27] V. G. Rousseau, Phys. Rev. E 77 (5) (2008) 056705.
[28] W. M. C. Foulkes, L. Mitas, R. J. Needs, G. Rajagopal, Rev. Mod. Phys. 73 (1) (2001) 33–83.
[29] M. Nightingale, C. J. Umrigar, (Eds.), Quantum Monte Carlo Methods in Physics and Chemistry, Kluwer, Dordrecht, 1999.

[30] H. Nakatsuji, Phys. Rev. A 72 (6) (2005) 062110.
[31] A. I. Streltsov, O. E. Alon, L. S. Cederbaum, Phys. Rev. Letters 99 (2007) 030402.
[32] O. E. Alon, A. I. Streltsov, L. S. Cederbaum, Phys. Rev. A 77 (2008) 033613.
[33] M. Nooijen, K. Shamasundar, D. Mukherjee, Mol. Phys. 103 (2005) 2277–2298.
[34] J. Schnack and P. Hage and H-J. Schmidt, J. Comp. Phys. 227 (2008) 4512–4517.
[35] P. J. Knowles, N. C. Handy, Comp. Phys. Commun. 54 (1989) 75.
[36] O. E. Alon and A. I. Streltsov and L. S. Cederbaum, Phys. Rev. A 77 (2008) 033613.
[37] A. I. Streltsov and K. Sakmann and O. E. Alon and L. S. Cederbaum, Phys. Rev. A 83 (2011) 043604.
[38] G. A. Meurant, The Lanczos and Conjugate Gradient Algorithms, SIAM, 2006.
[39] E. R. Davidson, J. Comp. Phys. 17 (1975) 87.
[40] Algorithms and Libraries for Physics Simulations, URL `http://alps.comp-phys.org/`, ????
[41] A. Albuquerque, F. Alet, P. Corboz, P. Dayal, A. Feiguin, S. Fuchs, L. Gamper, E. Gull, S. Gurtler, A. Honecker, R. Igarashi, M. Korner, A. Kozhevnikov, A. Lauchli, S. Manmana, M. Matsumoto, I. McCulloch, F. Michel, R. Noack, G. Pawłowski, L. Pollet, T. Pruschke, U. Schollwock, S. Todo, S. Trebst, M. Troyer, P. Werner, S. Wessel, J. of Magn. and Magn. Materials 310 (2007) 1187.
[42] O. Penrose, L. Onsager, Phys. Rev. 104 (1956) 576.
[43] Z. Rolik, Á. Szabados, P. R. Surján, J. Chem. Phys. 128 (2008) 144101.

Table 1: Occupation vectors (n_1, n_2, n_3) for $K = 3$ lattice sites and $N = 3$ particles. Addressing indices I are given for the lexicographical ordering as well as in the scheme used presently. In the last column, addressing for site occupation restricted at maximum $M = 2$ is shown.

			lexicographical	present	present, $M = 2$
n_1	n_2	n_3	I	I	I
3	0	0	1	1	–
2	1	0	2	2	1
1	2	0	4	3	2
0	3	0	7	4	–
2	0	1	3	5	3
1	1	1	5	6	4
0	2	1	8	7	5
1	0	2	6	8	6
0	1	2	9	9	7
0	0	3	10	10	–

Table 2: Total energies in units of t and energy error in round brackets, introduced by restricting maximal site occupation M, on the example of a square lattice with 4×4 sites (K=16) and $N = 16$ particles.

M	U/t	
	0.1	20
16 (unrestricted)	−50.7394205	−5.0515122
5	−50.3691777 (0.73 %)	−5.0515122 (0.00 %)
3	−46.6986081 (7.96 %)	−5.0513317 (0.02 %)
2	−37.1396387 (26.8 %)	−4.9857295 (1.31 %)

Figure 1: Ordinary Pascal's triangle (to the left) and generalized Pascal's triangle for $M = 2$ (to the right). Numbers in framed boxes give the dimension of the Hilbert space (unrestricted to the left, restricted to the right) for $N = 4$ particles and $K = 3$ sites.

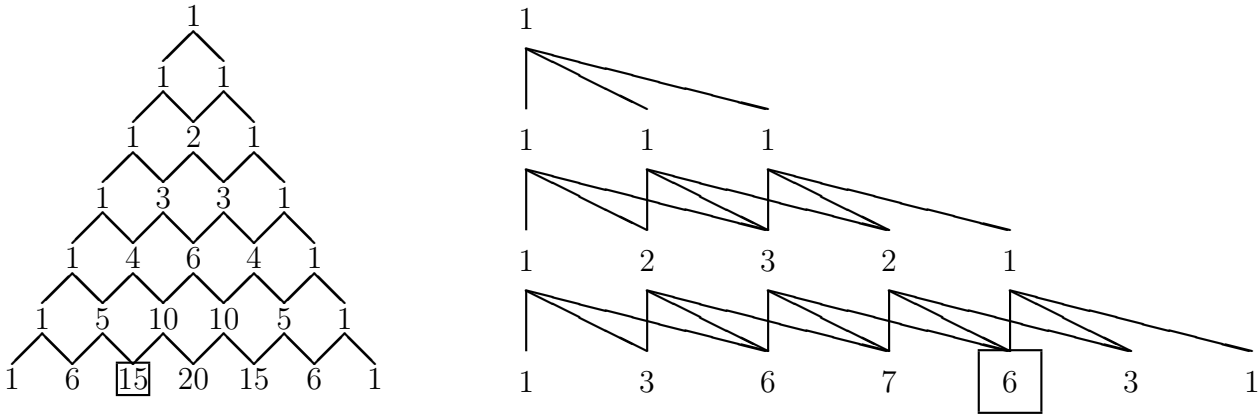

Figure 2: Memory and processor time required for reaching the ground state by the sparse Lanczos[40, 41] and by the present algorithm. A square lattice of 3×3 sites is assumed, number of particles N is varied on the horizontal axis.

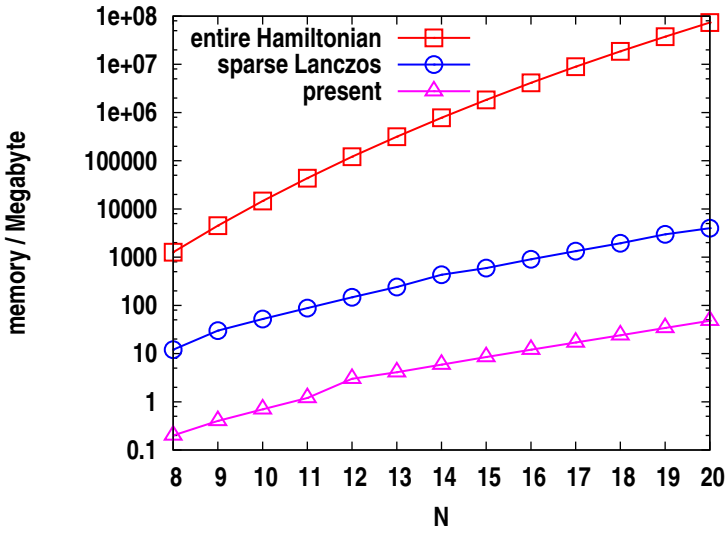

(a)

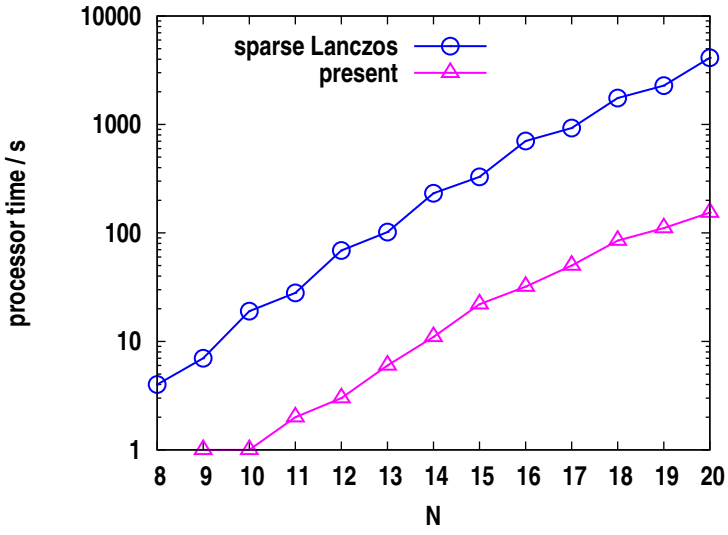

(b)

Figure 3: Expectation value of the particle number operator according to Eq.(21). A square lattice of 3×3 sites is assumed filled with $N = 9$ particles. The three panels show the three topologically different sites: (a) central, (b) on the edge, (c) on the corner. Results with restricted maximal site occupation, $M = 1, \ldots, 8$ are depicted along with full Hilbert space calculations (unrestricted).

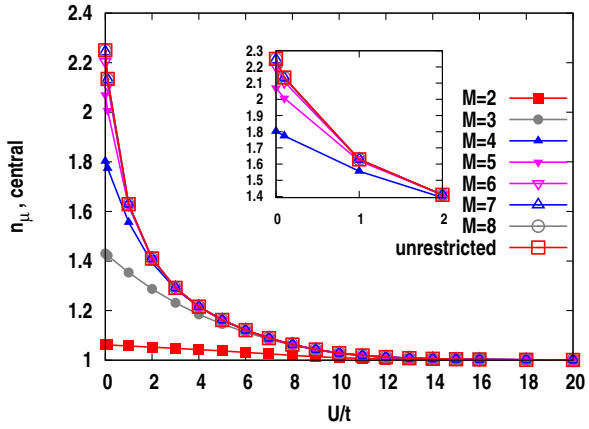

(a)

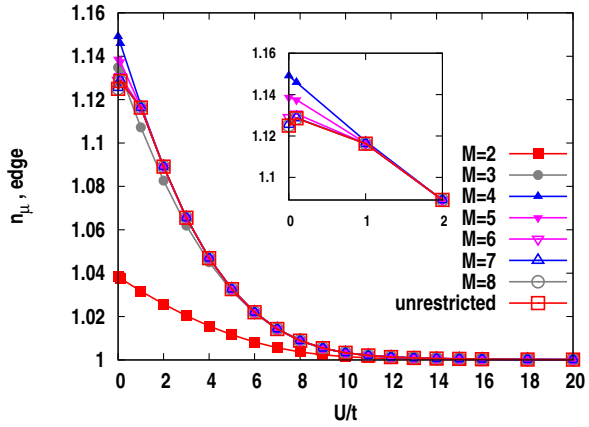

(b)

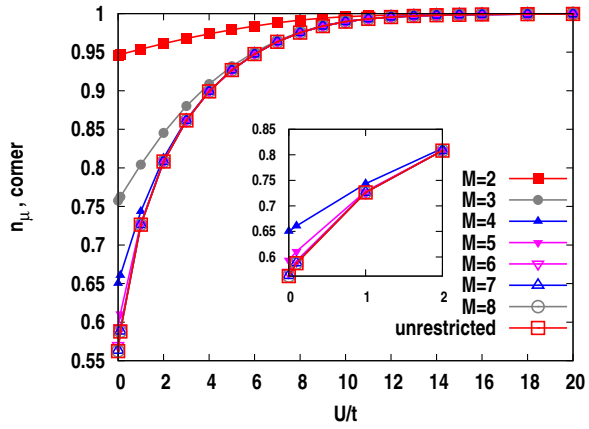

(c)

Figure 4: Variance of site occupation as computed by Eq.(22) on the example of a 3×3 lattice, filled with $N = 9$ particles. The three panels show the three topologically different sites: (a) central, (b) on the edge, (c) on the corner. Results with restricted maximal site occupation, $M = 1, \ldots, 8$ are depicted along with full Hilbert space calculations (unrestricted).

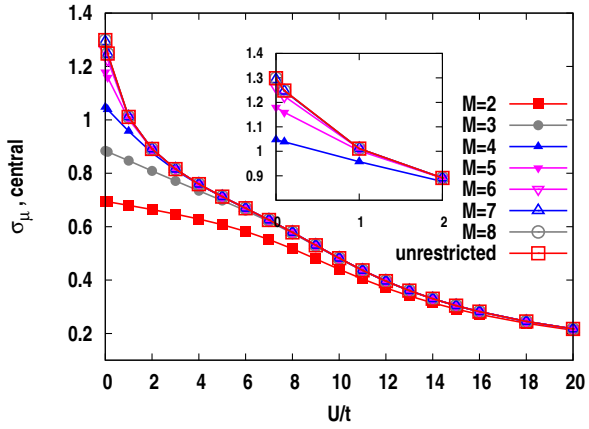

(a)

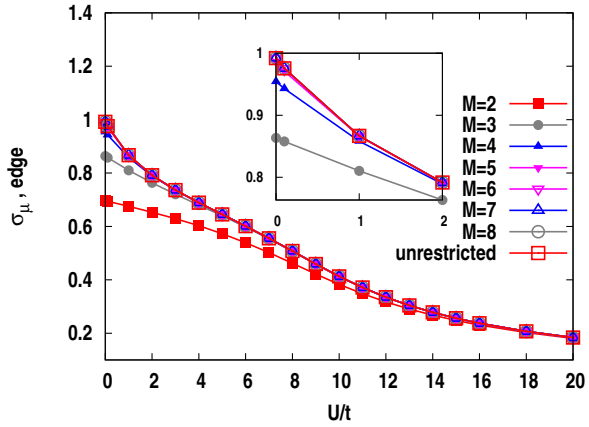

(b)

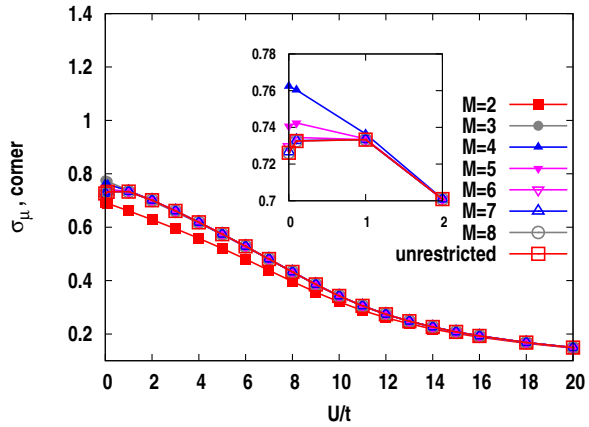

(c)

Figure 5: Condensate fraction (largest eigenvalue of the first order density matrix, divided by N) for a square lattice with 3×3 sites and $N = 9$ particles.

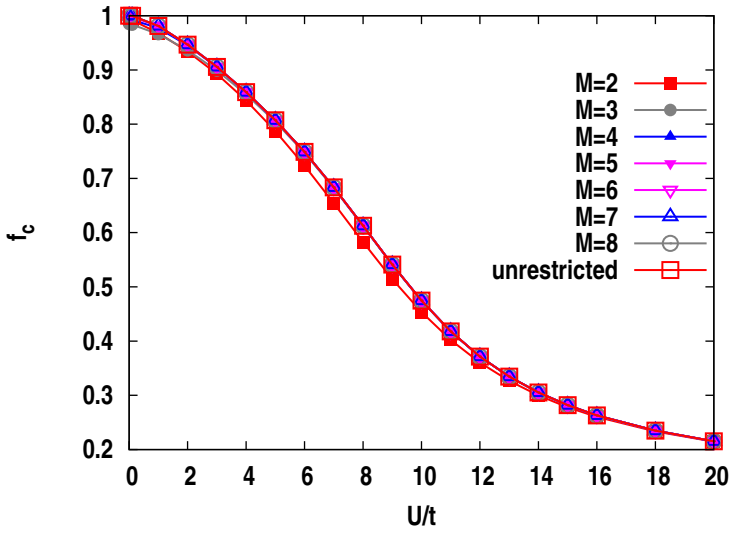

Table 3: Analysis on the sparsity of the CI vector for a square lattice with 4×4 sites (K=16) and $N = 16$ particles. Number of components above 10^{-n} in absolute value are tabulated. Diagonal to offdiagonal ratio of the first order density matrix $r = \left(\sum_i \rho_{ii}^2\right)^{1/2} / \left(\sum_{i \neq j} \rho_{ij}^2\right)^{1/2}$ is given in the first row.

U/t	0.1	1	10
r	0.094	0.079	0.328
$n = 1$	0	0	1
$n = 2$	0	0	$1.06{\cdot}10^{3}$
$n = 3$	$1.70{\cdot}10^{4}$	$2.47{\cdot}10^{4}$	$4.85{\cdot}10^{4}$
$n = 4$	$1.58{\cdot}10^{7}$	$1.60{\cdot}10^{7}$	$7.60{\cdot}10^{5}$
$n = 5$	$1.01{\cdot}10^{8}$	$9.55{\cdot}10^{7}$	$5.07{\cdot}10^{6}$
$n = 6$	$1.15{\cdot}10^{8}$	$1.05{\cdot}10^{8}$	$1.70{\cdot}10^{7}$
below 10^{-6}	$6.90{\cdot}10^{7}$	$8.41{\cdot}10^{7}$	$2.78{\cdot}10^{8}$